Constructing the Universe with Clusters of Galaxies, IAP 2000 meeting, Paris (France) July 2000
Florence Durret & Daniel Gerbal eds.

LARGE-SCALE DISTRIBUTION and SPECTRAL PROPERTIES of GALAXIES in the SHAPLEY CONCENTRATION

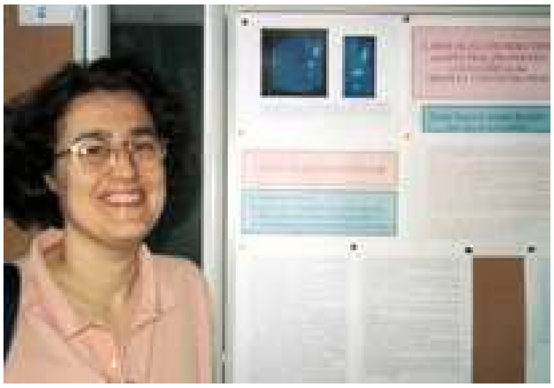

ELENA ZUCCA & SANDRO BARDELLI
Osservatorio Astronomico di Bologna, via Ranzani 1, I-40127 Bologna, Italy
A.BALDI, G.ZAMORANI, L.MOSCARDINI, R.SCARAMELLA

We present the results of a redshift survey of both cluster and intercluster galaxies in the central part of the Shapley Concentration, the richest supercluster of clusters in the nearby Universe, consisting of ~ 2000 radial velocities. We estimate the total overdensity in galaxies of the supercluster and its mass and we discuss the cosmological implications of these results. Moreover, using a Principal Components Analysis technique, we study the influence of the cluster and supercluster dynamics on the galaxy spectral morphology.

Clusters of galaxies are thought to form by accretion of subunits in a hierarchical bottom up scenario: numerical simulations revealed that mergings happen along preferential directions, called density caustics, which define matter flows, at whose intersection rich clusters are formed. The central regions of rich superclusters, where the overdensity is of the order of ~ 10, are thought to be in the early collapse phase and therefore give the possibility to study the formation of clusters and groups of galaxies. These regions are the ideal environment for the detection of cluster mergings, because the peculiar velocities induced by the enhanced local density of the large scale structure favour the cluster-cluster and cluster-group collisions, in the same way as the caustics seen in the simulations.
Spectacular major merging events are visible in the central region of the Shapley Concentration, the richest supercluster of galaxy clusters in the nearby Universe (Zucca et al. 1993). Particularly interesting are two chains of interacting clusters: the A3558 and the A3528 complexes (Fig. 1). We are carrying on a long term multiwavelength study on the Shapley Concentration (see also the poster by Bardelli et al., these proceedings), in order to determine its mass, dynamical state and cosmological relevance, as well as to analyse in detail the physics of the merging phenomena. In this poster we focus on the large-scale distribution and spectral properties of galaxies both in clusters and in the "field" in between clusters.

1 Large-scale distribution of galaxies

In collaboration with G.Zamorani, L.Moscardini, R.Scaramella
The distribution of clusters inside the Shapley Concentration is quite well studied; on the contrary, little is known about the distribution and the overdensity of intercluster galaxies.

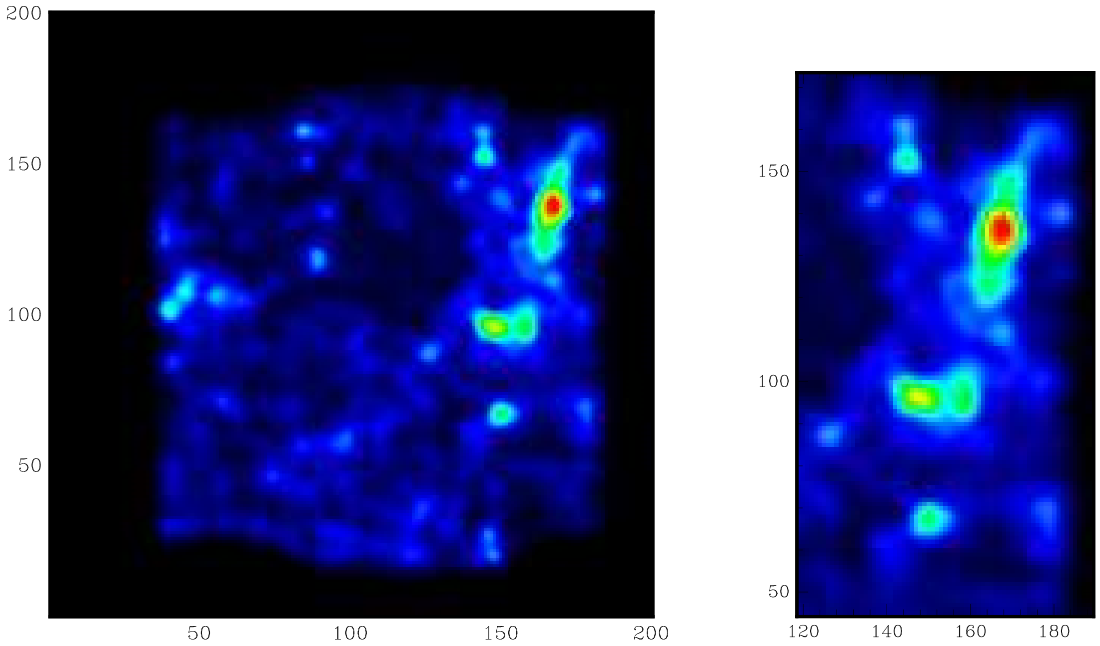

The A3528 complex

Isodensity contours of the optical bidimensional distribution of galaxies with $b_J \leq 19.5$ in the UKSTJ plate 443. In the upper right part of the figure there is the A3528 complex, formed by A3528, A3530 and A3532. On the right, a zoom of the complex, which appears elongated in the North-South direction, is shown.

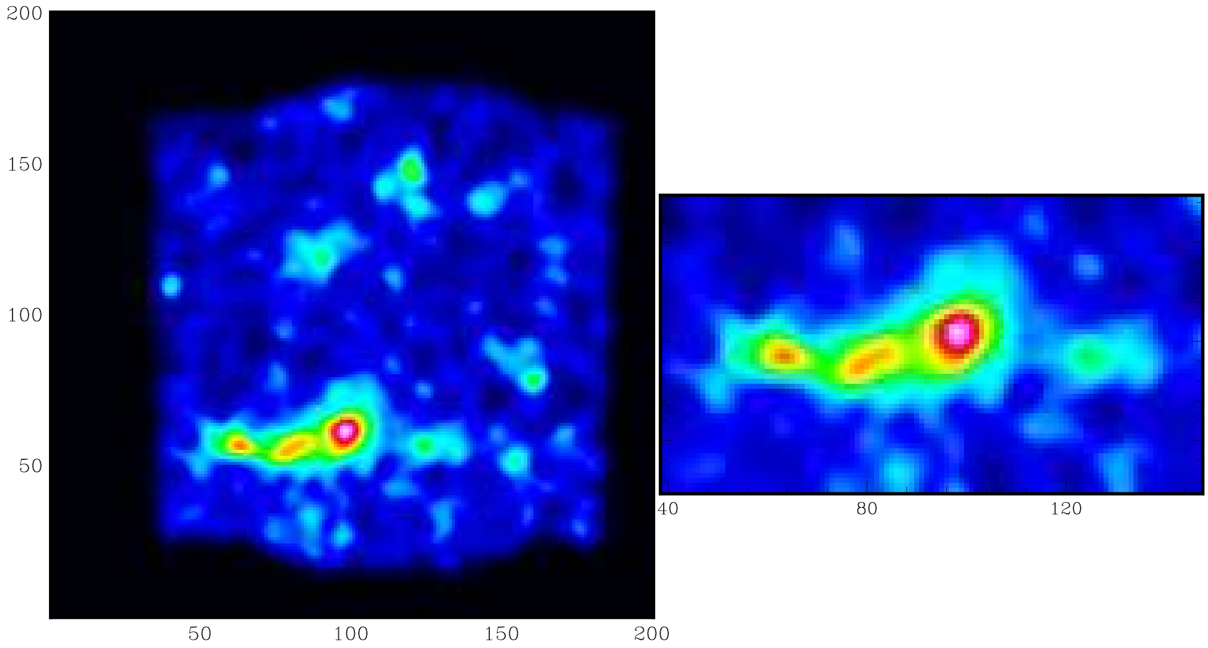

The A3558 complex

Isodensity contours of the optical bidimensional distribution of galaxies with $b_J \leq 19.5$ in the UKSTJ plate 444. In the lower left part of the figure there is the A3558 complex, formed by A3558, A3556 and A3562. On the right, a zoom of the complex, which appears elongated in the East-West direction, is shown.

Figure 1: Optical distribution of galaxies in the central part of the Shapley Concentration.

For this reason we performed a redshift survey of galaxies which are outside the clusters and the obvious bi–dimensional overdensities in this region, in order to derive the distribution and the overdensity of "field" objects. These data have been added to our surveys covering the cluster complexes (Bardelli et al. 1994, 1998a, 2000b), resulting in a total redshift sample of ~ 2000 radial velocities. In Figure 2 we show our sampling strategy: big and small circles correspond to the field of view of the MEFOS and OPTOPUS multifiber spectrographs (at the 3.6m ESO telescope), respectively.

In Figure 3 we show the wedge diagram of our sample. It is clear the presence of the two cluster complexes dominated by A3558 (on the left) and by A3528 (on the right). These two structures appear to be connected by a bridge of galaxies, resembling the Coma-A1367 system, the central part of the Great Wall. The scale of this system is ~ 23 h^{-1} Mpc and it is comparable to that of Coma-A1367 (~ 21 h^{-1} Mpc). Note the presence of two voids at ~ 20000 km/s and ~ 30000 km/s in the easternmost half of the wedge, labelled as V1 and V2 respectively. Other two voids (V3 and V4) are visible in the westernmost part of the plot: in particular, void V3 appears to be delimited by two elongated features (S300a and S300b) which appear to "converge" in a single feature at right ascension $\sim 13^h$ (S300c). We refer to this structure with the name S300: as shown below, the overdensity corresponding to this excess is remarkably high.

Our main results are the following (Bardelli et al. 2000a):

– The average velocity of the observed intercluster galaxies in the Shapley Concentration appears to be a function of the (α, δ) position, and can be fitted by a plane in the three–dimensional space (α, δ, v): the distribution of the galaxy distances around the best fit plane is described by a Gaussian with $\sigma = 3.8$ h^{-1} Mpc .

– Using the 1440 galaxies of our sample in the magnitude range $17 - 18.8$, we reconstructed the density profile in the central part of the Shapley Concentration and we detected another significant overdensity at ~ 30000 km/s (see Figure 4).

– We estimate the total overdensity in galaxies, the mass and the dynamical state of these structures, discussing the effect of considering a bias between the galaxy distribution and the underlying matter. The estimated total overdensity in galaxies of these two structures is $\frac{N}{\bar{N}} \sim 5.2$ on scale of 15.5 h^{-1} Mpc for the Shapley Concentration and $\frac{N}{\bar{N}} \sim 2.9$ on scale of 24.8 h^{-1} Mpc for S300. If light traces the mass distribution, the corresponding masses are 2.3×10^{16} Ω h^{-1} $M_\odot$ and 5.1×10^{16} Ω h^{-1} $M_\odot$ for Shapley Concentration and S300, respectively (see Table 1 and Figure 5).

The dynamical analysis reveals that, if light traces mass and $\Omega = 1$, the Shapley Concentration already reached its turnaround radius and started to collapse: the final collapse will happen in $\sim 3\ 10^9$ h^{-1} yrs.

– We compare our mass estimates on various scales with other results in the literature, finding a general agreement (see Figure 5).

– We find an indication that the value of the bias between clusters and galaxies in the Shapley Concentration is higher than that reported in literature, confirming the impression that this supercluster is very rich in clusters.

– Finally from the comparison with some theoretical scenarios, we find that the Shapley Concentration is consistent with the predictions of the models with more power on large scale (such as Open and Λ CDM), while it is inconsistent with the standard CDM normalized to the cluster abundance.

2 Spectral properties of galaxies

In collaboration with A.Baldi

The large amount of spectra in our sample allows a uniform spectral classification of galaxies

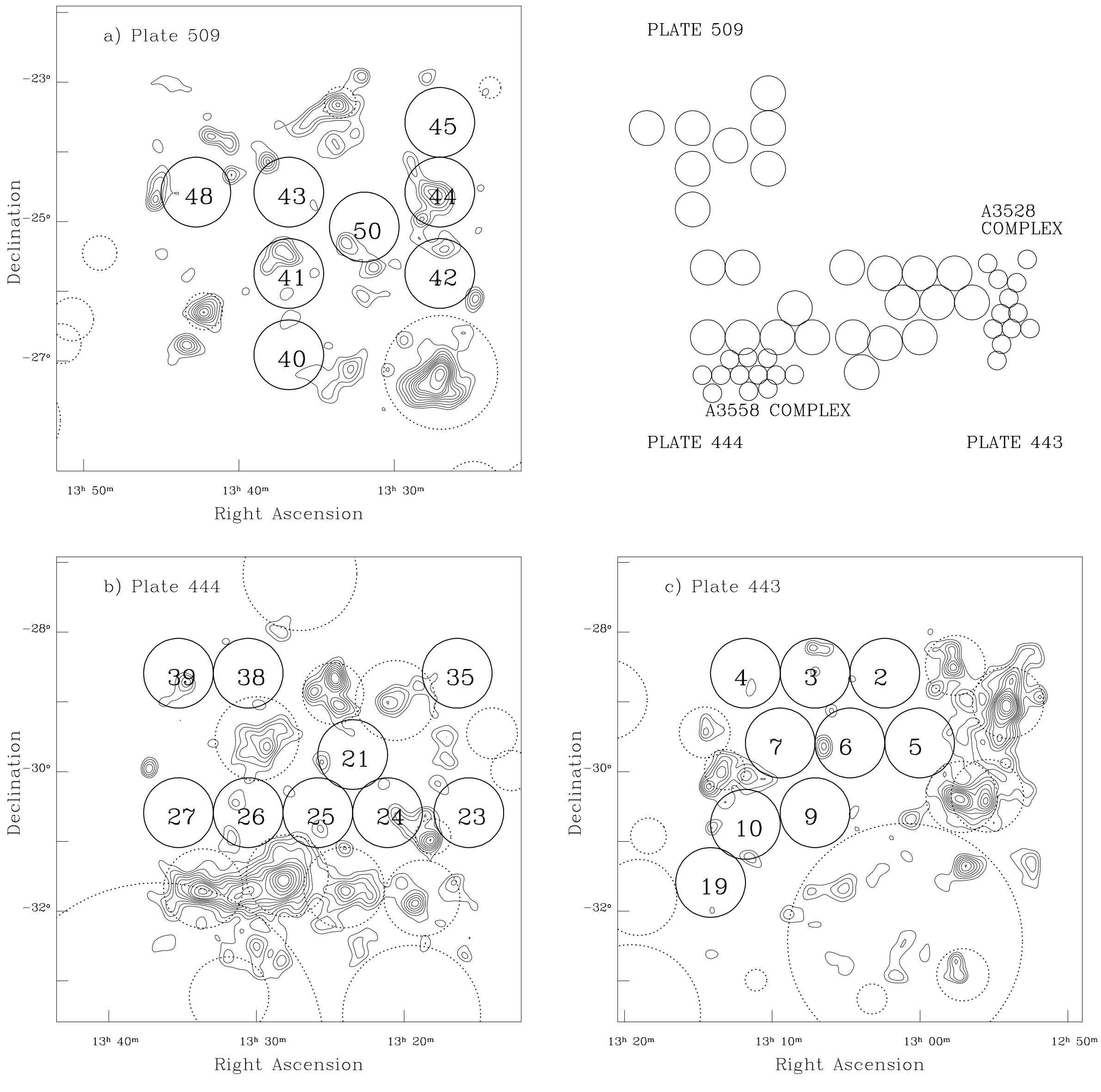

Figure 2: Isodensity contours of the bidimensional distribution of the galaxies in the b_J magnitude bin $17-19.5$ in the UKSTJ plates which cover the central part of the Shapley Concentration. For the Abell clusters present in the plates, circles of one Abell radius have been drawn (dashed curves). Solid circles represent the MEFOS fields.

a) Plate 509; b) Plate 444; c) Plate 443. The two most evident systems are the A3558 (plate 444) and the A3528 (plate 443) cluster complexes. The dashed circle at the bottom right corner of plate 509 corresponds to the cluster A1736.

The relative positions of the fields is shown in the upper right panel, where small circles represent OPTOPUS observations on the cluster complexes.

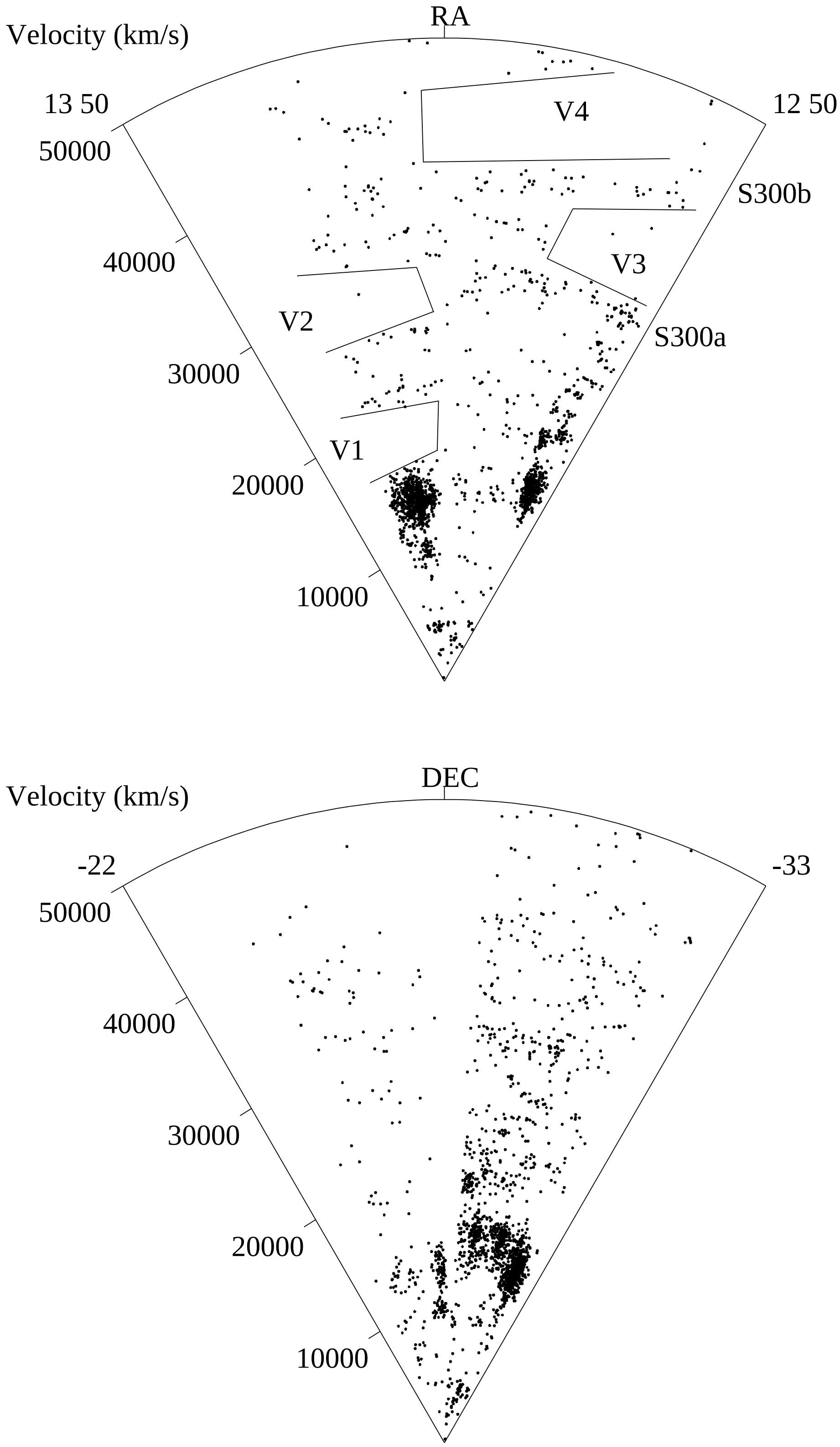

Figure 3: Wedge diagram of the galaxy distribution in our samples. Upper panel: 1728 galaxies in the plates 444 and 443 and in the velocity range [0 – 50000] km/s. Note the clear presence of the A3558 and A3528 complexes and of four voids. Lower panel: 1979 galaxies in plates 443, 444 and 509 in the velocity range [0-50000] km/s. Note that the plotted coordinate is the declination.

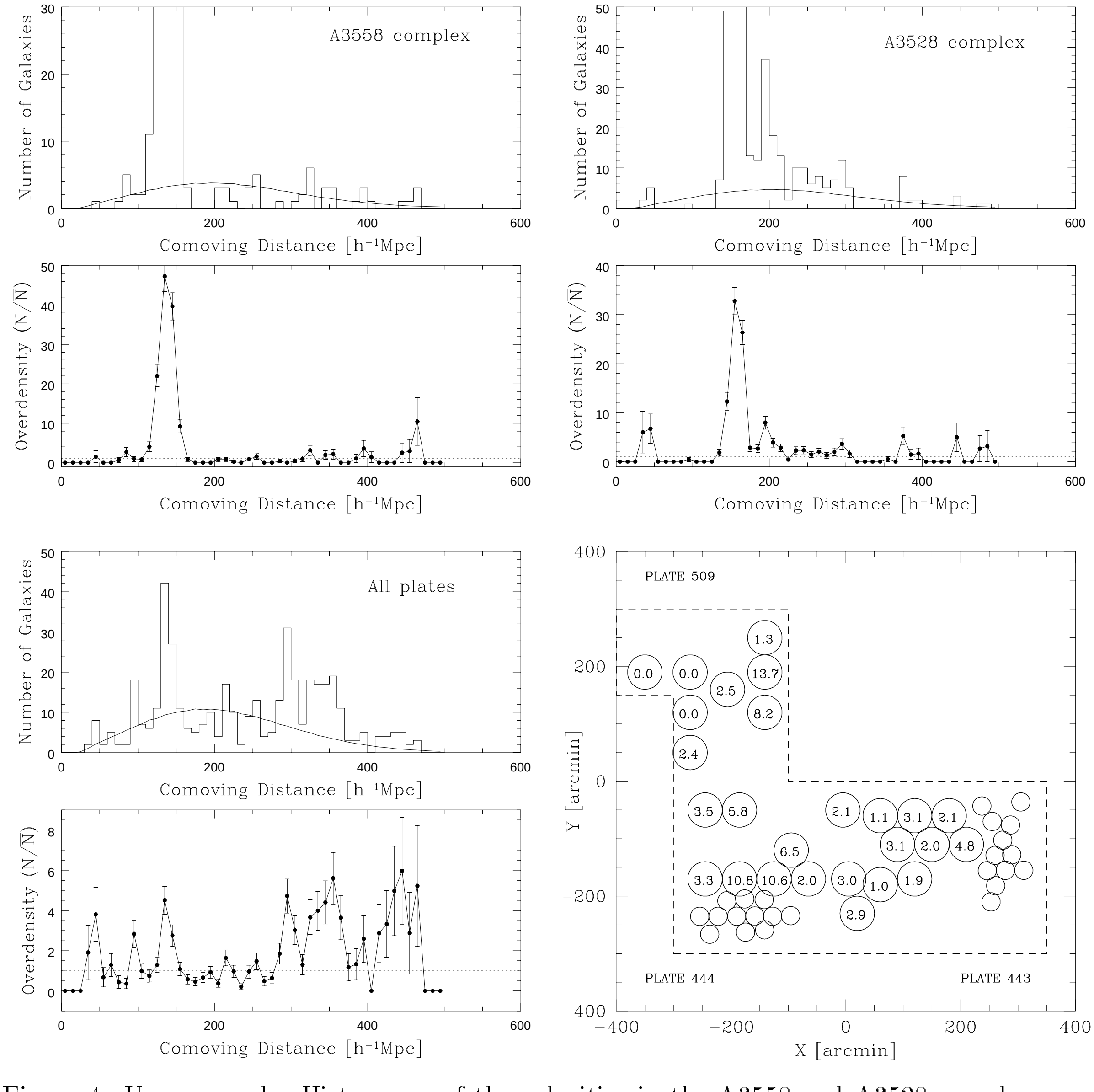

Figure 4: Upper panels: Histograms of the velocities in the A3558 and A3528 complexes and in the intercluster sample, with superimposed the distribution expected for a uniform sample. Lower panels: Galaxy density profiles. The dotted line corresponds to $\frac{N}{\bar{N}} = 1$. The estimated overdensities in the single MEFOS fields as distributed in the sky are reported in the last figure.

Table 1: Estimated overdensities for the samples in the Shapley Concentration

Sample	Overdensity $\frac{N}{\bar{N}}$	Volume [h^{-3} Mpc^3]	Scale [h^{-1} Mpc]	Mass [Ω_o h^{-1} $M_\odot$]
A3558 complex	46.4 ± 2.4	415.6	4.6	$5.4\ 10^{15}$
A3528 complex	21.4 ± 1.2	609.5	5.3	$3.6\ 10^{15}$
A1736	19.7 ± 3.1	247.8	3.9	$1.4\ 10^{15}$
Intercluster sample	3.9 ± 0.4	3082.8	9.0	$3.3\ 10^{15}$
Total sample	11.3 ± 0.4	4355.8	10.1	$1.4\ 10^{16}$
Extended sample	6.8 ± 0.4	11611.3	14.1	$2.2\ 10^{16}$
Extended sample+382&383	5.2 ± 0.3	15607.8	15.5	$2.3\ 10^{16}$

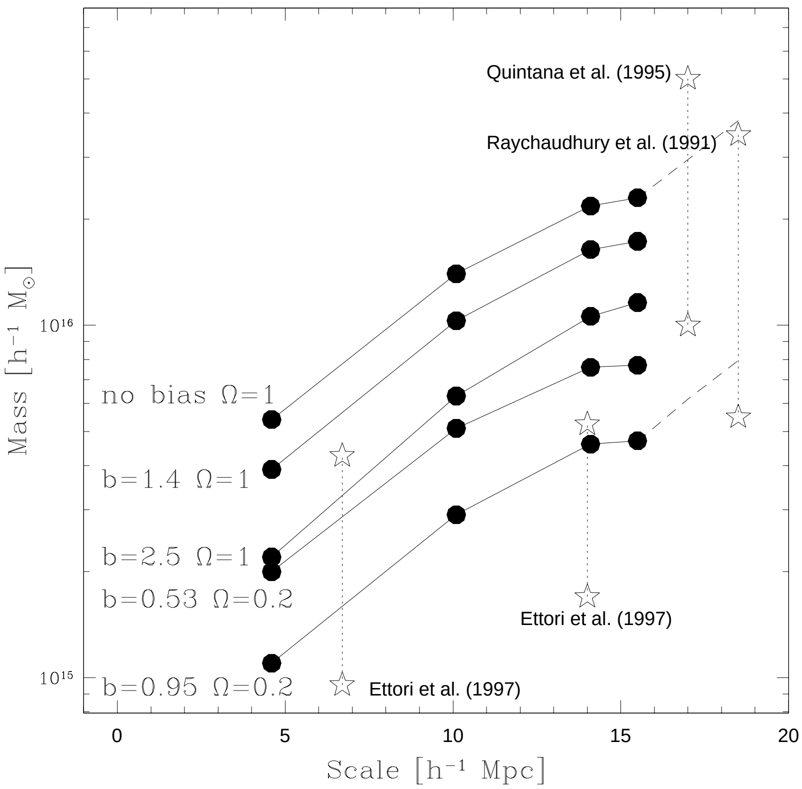

Figure 5: Estimated masses at various scales for different parameter choices, indicated near each curve. Stars connected with dotted lines refer to mass ranges given in the literature. Dashed lines give the extrapolation of our mass values to the scales of Quintana et al. and Raychaudhury et al., assuming the same overdensity we found at our largest scale.

The overdensity and mass values for various sample are reported in the Table. The case "Total sample" includes all regions spectroscopically observed by us; the case "Extended sample" assumes that the estimated overdensity extends also outside MEFOS fields, over the whole plates 443, 444 and 509; the case "Extended sample + 382 & 383" is obtained adding also the overdensity values found by Drinkwater et al. (1999) for plates 382 and 383.

in the Shapley Concentration, in order to investigate the morphology–density relation in a wide range of densities, from the cluster to the supercluster environment, in this dynamically active region (Baldi, Bardelli & Zucca, 2000).
The method we have chosen to perform spectral classification of our sample of galaxies is the Principal Components Analysis, following the Galaz & deLapparent (1998) paper.
We have considered only galaxies in the velocity range $10000 - 22500$ km/s, in order to limit the spectral analysis to the physical extension of the Shapley Concentration. Moreover, given the fact that the intercluster survey is limited to the the magnitude range $17 \leq b_J \leq 18.8$, when we compare the cluster galaxy properties with the intercluster ones, we use subsamples with these magnitude limits. Our final sample contains $\sim$ 800 spectra.
Note that, although fiber spectra do not allow a very precise flux calibration, in our case the use of a limited distance range maintains the spectral features at approximately the same wavelength and therefore at the same instrumental response.
In order to have a comparison of supercluster spectra with those of "true" field galaxies, we have considered a sample taken from the ESO Slice Project (ESP) galaxy redshift survey (Vettolani et al. 1997). This survey was obtained with the same telescope and instrumental set up of our sample and therefore represents a well defined reference sample.
From the PCA analysis, we found that the first three principal components (PCs) (reported in Figure 6) are sufficient to reconstruct $\sim$99% in flux of the sample. Then, following Galaz & deLapparent (1998), we applied a coordinate trasformation from the three-dimensional space defined by the PCs to the bi-dimensional space (δ, θ). The δ parameter represents the importance of the blue part of the continuum with respect to the red one, while θ is an indicator of the emission line strength in a galaxy spectrum.
The galaxies follow a well defined sequence in the (δ, θ) plane (Figure 6) and the Kennicutt's galaxies (of known morphological type) are located in a succession of increasing values of δ, going from the ellipticals to the irregulars. For this reason, in the following we'll use δ to classify galaxies.
In Figure 7 the fractions of galaxies in three morphological bins (early, intermediate and late type) are shown for each sample. As expected, cluster galaxies show a completely different morphological distribution with respect to ESP and intercluster galaxies, being the fraction of early-type galaxies dominant in such high density environment.
More interesting, this figure shows a broad agreement between the intercluster and the ESP sample: this fact suggests that the galaxies located in the intercluster regions of the Shapley supercluster have a morphological mix not different from field galaxies.
Looking at the dependence of the morphological mix on the local density (Figure 7), a decreasing of the late-type galaxies fraction with increasing values of density is clearly visible, both in the A3528 and in the A3558 complexes, reflecting the well-known morphology–density relation. Moreover, for every density value, this fraction remains significantly below the mean field value. From the A3528 complex, we have eliminated galaxies belonging to the poor cluster A3535 (which is not dynamically part of the structure): the morphological mix of these objects remains almost constant with the density and with values in agreement with those found for the field population.
The spatial distribution of early-type and late-type galaxies in the two cluster complexes is shown in Figure 8.
In Figure 9 we show the dependence of the mean [OII] equivalent width and of the mean star formation rate (derived following Kennicut 1992) on the local density.

References

1. Baldi A., Bardelli S., Zucca E., 2000, MNRAS submitted

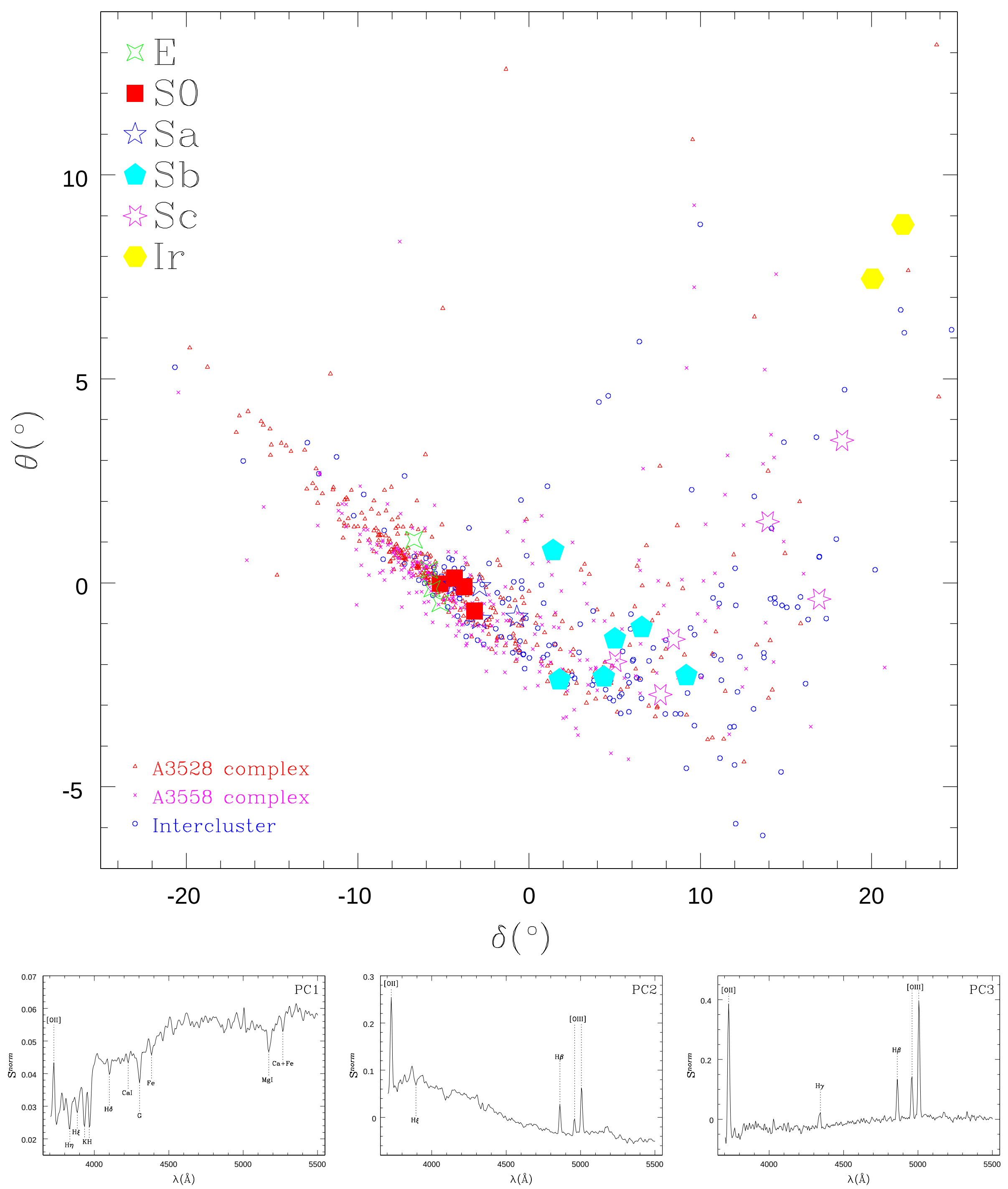

Figure 6: The classification diagram δ-θ for the spectral sample in the Shapley Concentration plus the Kennicutt's sample (big symbols). The first three principal components (PCs) obtained from the PCA analysis are shown in the lower panel.

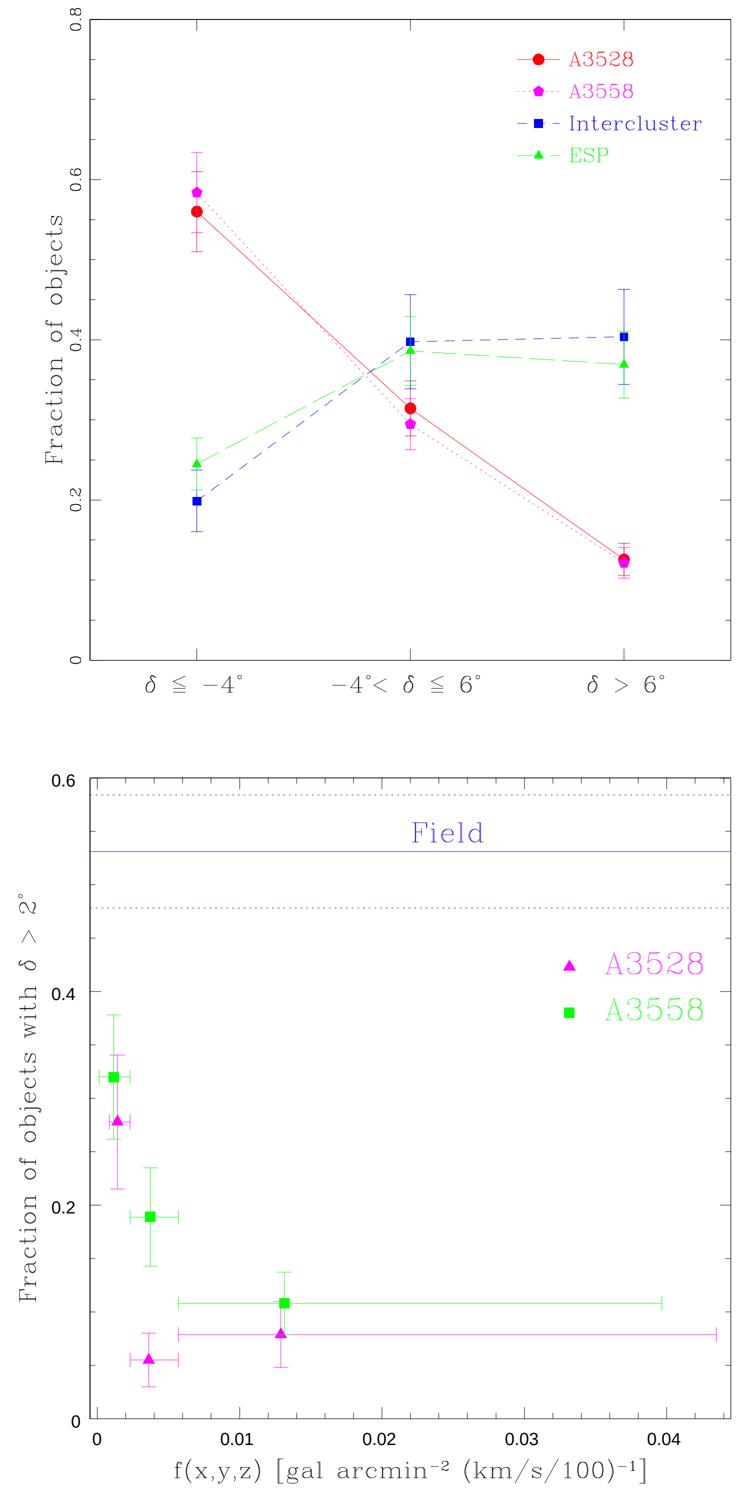

Figure 7: Upper panel: Fractions of galaxies divided in three morphological classes, for each spectral sample: A3528 (circles), A3558 (pentagons), intercluster (squares) and ESP (triangles). Lower panel: Relation between the fraction of late-type galaxies and local density $f(x, y, z)$ in the A3528 (triangles) and A3558 (squares) complexes, in the magnitude range $17.0 \leq b_J \leq 18.8$. Horizontal bars indicate the extension of the density intervals: the points are located at the position of the density average value within the bin. Vertical bars represent the 1-σ uncertainties. The reference value for the field (from ESP galaxies) is reported as a solid line: dotted lines represent its 1-σ uncertainties.

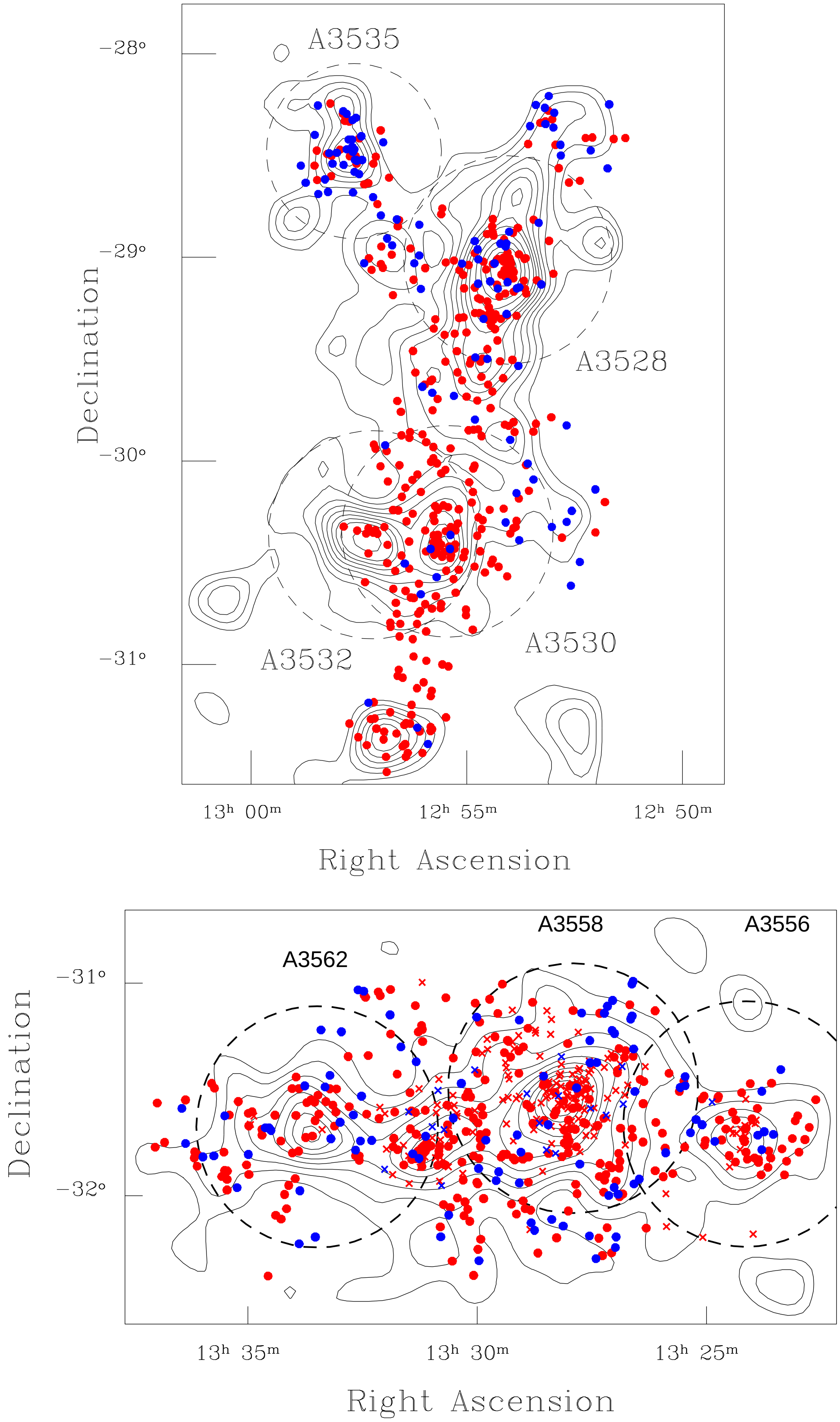

Figure 8: Spectral classification of galaxies superimposed to the isodensity contours in the cluster complexes. Red dots: early-type galaxies. Blue dots: late-type galaxies. Upper panel: A3528 complex. Lower panel: A3558 complex (in this panel, crosses indicate objects for which the classification has been derived from literature $(U-B)$ colors).

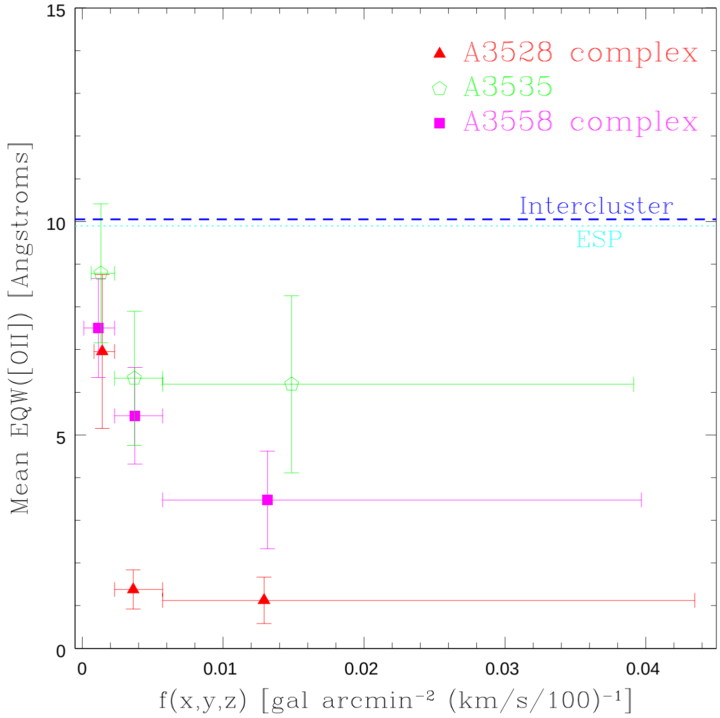

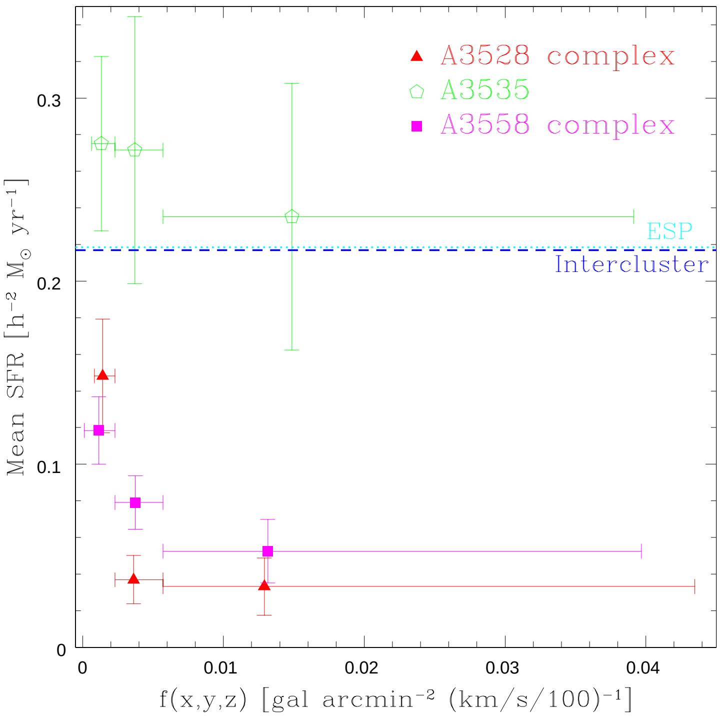

Figure 9: Upper panel: Relation between the mean [OII] equivalent width and the local density $f(x, y, z)$ in the A3528 (triangles) and A3558 (squares) complexes, in the magnitude range $17.0 \leq b_J \leq 18.8$. The meaning of the intervals is the same as Figure 2. The A3535 cluster has been considered separately, because it is not dynamically part of the A3528 complex. The horizontal blue line represents the reference value for the field. Lower panel: Relation between the mean star formation rate (derived following Kennicut 1992) and the local density $f(x, y, z)$, for the same samples.

2. Bardelli S., Zucca E., Vettolani G., Zamorani G., Scaramella R., Collins C.A., MacGillivray H.T., 1994, MNRAS 267, 665
3. Bardelli S., Zucca E., Malizia A., Zamorani G., Scaramella R., Vettolani G., 1996, A&A 305, 435
4. Bardelli S., Zucca E., Zamorani G., Vettolani G., Scaramella R., 1998a, MNRAS 296, 599
5. Bardelli S., Pisani A., Ramella M., Zucca E., Zamorani G., 1998b, MNRAS 300, 589
6. Bardelli S., Zucca E., Zamorani G., Moscardini L., Scaramella R., 2000a, MNRAS 312, 540
7. Bardelli S., Zucca E., Baldi A., 2000b, MNRAS in press (astro-ph/0009008)
8. Drinkwater M.J., Proust D., Parker Q.A., Quintana H., Slezak E., 1999, PASA 16, 113
9. Galaz G., de Lapparent V., 1998, A&A 332, 459
10. Kennicutt R.C., 1992, ApJ 388, 310
11. Vettolani G., Zucca E., Zamorani G. et al., 1997, A&A 325, 954
12. Zucca E., Zamorani G., Scaramella R., Vettolani G., 1993, ApJ 407, 470
13. Updates to this project: http://boas5.bo.astro.it/~bardelli/shapley/shapley_new.html